

Effects of Heat-Treatment on the High-Temperature Ductility and Fracture of 20 Cr/25 Ni/Nb Stabilised Austenitic Steel

A. GITTINS*

Materials Division, Central Electricity Research Laboratories, Leatherhead, Surrey, UK

Stabilisation of 20 Cr/25 Ni steel by niobium not only increased the creep resistance but eliminated the tendency for cracking and thereby enhanced the ductility. No change in density was detected in fine-grained specimens solution-treated at 1000° C until well into tertiary creep, and elongations of 75 to 150% were obtained. After a solution-treatment at 1250° C the creep resistance was further increased and denuded zones were formed near grain boundaries. This caused the strain to be concentrated in grain boundary regions during creep, leading to the formation of both surface- and wedge-cracks at grain boundaries. However, in contrast to a niobium-free steel, these did not nucleate until the end of the secondary creep.

1. Introduction

In a recent investigation [1] density measurements were used to study the development of triple-point cracks during creep in an unstabilised 20 Cr/25 Ni stainless steel. It was found that cracks were nucleated at creep strains of < 1% and that they grew at a rate proportional to the duration of creep raised to the power of three. This rapid growth rate limited the ductility to ~ 25% in fine-grained specimens and to ~ 10% in coarse-grained specimens. The effect of niobium additions on the creep ductility of 20 Cr/25 Ni stainless steel is uncertain although in hot tensile tests at 750°C both the unstabilised [2] and the niobium-stabilised [3] steels gave ductilities of 55 to 60%. (However, metallographic observation of fractured specimens showed that wedge-cracking was common only in the unstabilised steel.) Because of the importance of ductility in the use of 20 Cr/25 Ni/Nb stainless steels as a canning material for gas-cooled nuclear reactors, it was decided to study how the ductility of this steel is related to the tendency for the material to develop cavities during creep. With this object in view, creep tests were carried out after annealing specimens under conditions that lead to either high or low

ductility and the incidence of cavitation was recorded by density measurements. Where appropriate, the behaviour of the steel will be compared with the unstabilised steel studied in the earlier investigation.

2. Experimental Methods and Results

2.1. Material

The composition of the alloy used in this investigation, together with the Nb:C + N ratio, is shown in table I:

The amount of Nb is sufficient to stabilise all

TABLE I Chemical composition (wt %) of steel

Chromium	20.1
Nickel	24.9
Carbon	0.045
Niobium	0.65
Manganese	0.63
Silicon	0.62
Boron	0.0005
Nitrogen	0.007
Sulphur	0.005
Phosphorus	0.005
Titanium	0.05
Aluminium	0.05
Nb/(C + N) ratio	12.5:1

*Now at Broken Hill Proprietary Co Ltd, Melbourne Research Laboratories, Clayton, Victoria, Australia.

TABLE II Summary of creep tests

Specimen number	Heat-treatment (all air-cooled)	Grain size, μm	Test temp, $^{\circ}\text{C}$	Stress, MN m^{-2}	Sec. creep rate, h^{-1}	Time to fracture, h	Ductility %	Comments
1	1 h 1000 $^{\circ}\text{C}$, 20 h 820 $^{\circ}\text{C}$	30	704	62	2.5×10^{-5}	—	—	test stopped at 2%
2	1 h 1000 $^{\circ}\text{C}$, 20 h 820 $^{\circ}\text{C}$	30	736	62	2.0×10^{-4}	~ 800	> 105	necked, unbroken
3	1 h 1000 $^{\circ}\text{C}$, 20 h 820 $^{\circ}\text{C}$	30	750	62	6.5×10^{-4}	381	80	tested <i>in vacuo</i>
3a	1 h 1000 $^{\circ}\text{C}$, 20 h 820 $^{\circ}\text{C}$	30	750	62	6.2×10^{-4}	378	75	tested in air
4	1 h 1000 $^{\circ}\text{C}$, 20 h 820 $^{\circ}\text{C}$	30	777 $\frac{1}{2}$	62	2.4×10^{-3}	~ 135	> 85	unbroken
5	1 h 1000 $^{\circ}\text{C}$, 20 h 820 $^{\circ}\text{C}$	30	750	93	9.7×10^{-3}	44	149	broken, double neck
6	2 h 1250 $^{\circ}\text{C}$, 20 h 820 $^{\circ}\text{C}$	250	750	62	6.5×10^{-5}	—	—	stress increased to 93 MN m^{-2} after 1% strain
				93	3.3×10^{-4}	450	27	intergranular fracture, no necking
7	2 h 1250 $^{\circ}\text{C}$, 20 h 1050 $^{\circ}\text{C}$	250	750	62	1.2×10^{-4}	2808	41	tested to 10.6% <i>in vacuo</i> (942 h) then in air

the carbon as NbC. Apart from the C and Nb content, this steel is similar to the one used previously [1].

2.2. Heat-treatment and Microstructure of Specimens

Before creep-testing, specimens were given a variety of heat-treatments (table II), designed to produce differences in both NbC dispersion and grain size. According to Deighton [4], the solubility of carbon in 20 Cr/25 Ni/Nb austenite increases with temperature as shown in table III.

TABLE III Solubility of carbon in 20 Cr/25 Ni/Nb steel [4]

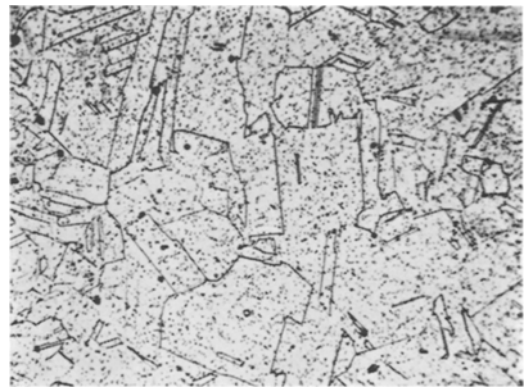
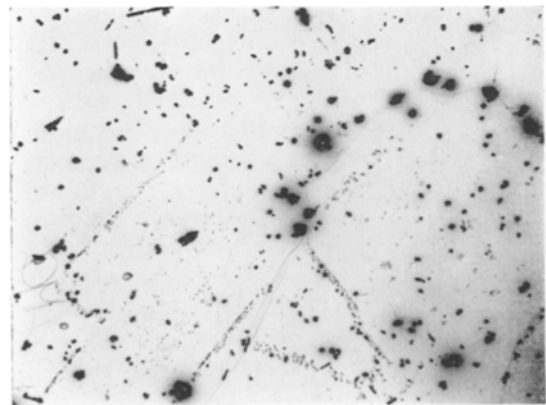
Temp, $^{\circ}\text{C}$	Solubility of C, %
820	< 0.002
1000	0.006
1050	0.010
1250	0.065

Thus for a carbon level of 0.045% most of the carbon will be out of solution below 1050 $^{\circ}\text{C}$ and grain growth will be suppressed. Ageing at 820 $^{\circ}\text{C}$ will precipitate most of the remaining carbon.

Typical microstructures of specimens 1 to 5 (table II) solution-treated at 1000 $^{\circ}\text{C}$ and aged at 820 $^{\circ}\text{C}$ are shown in figs. 1 and 2. The NbC is present as coarse particles undissolved by solution-treatment at 1000 $^{\circ}\text{C}$ and also as fine particles that may have precipitated during ageing.

All the NbC is dissolved at 1250 $^{\circ}\text{C}$ and grain

growth occurs. The dispersion of NbC precipitated by annealing below 1250 $^{\circ}\text{C}$ depends on the

Figure 1 Dispersion of NbC in 20 Cr/25 Ni/Nb stainless steel after 1 h 1000 $^{\circ}\text{C}$ AC, 20 h 820 $^{\circ}\text{C}$ AC ($\times 338$).Figure 2 As fig. 1 carbon extraction replica ($\times 513$).

temperature. Ageing at 820° C produces a fine rosette dispersion of NbC particles (identified by electron diffraction) $\sim 0.1 \mu\text{m}$ in diameter (fig. 3), although near the grain boundaries the NbC particles are coarser and denuded zones are present (fig. 4). The NbC dispersion formed by annealing at 1050° C after solution-treatment at 1250° C is similar to that found in fine-grained specimens.

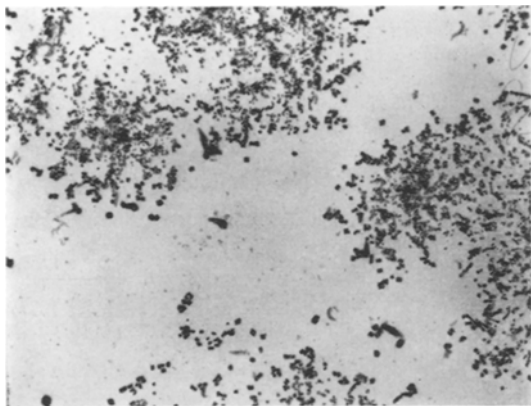


Figure 3 20 Cr/25 Ni/Nb stainless steel after 2h 1250° C AC, 20 h 820° C AC. Carbon extraction replica showing colonies of NbC ($\times 5194$).

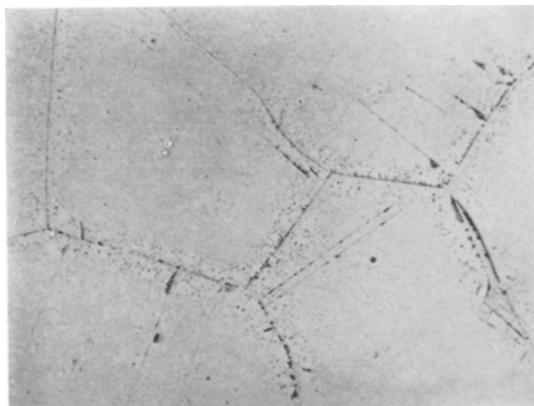


Figure 4 Denuded zones and coarse NbC precipitation in boundary regions of coarse-grained 20 Cr/25Ni/Nb steel ($\times 206$).

2.3. Creep Data

Creep tests were carried out mostly *in vacuo* using the techniques described previously [1]. In fig. 5 the creep curve of the fine-grained niobium-stabilised steel at 750° C 62 MN m⁻² is compared with the niobium-free steel used in the previous

investigation. (Both steels had the same grain size and heat-treatment.) An increase in carbon from 0.015 to 0.045 wt % and addition of 0.66 wt % Nb resulted in a marked increase in both creep-resistance and ductility. The ductility of all the fine-grained specimens was at least 75% (table II) and considerable necking preceded fracture. No significance is attached to the differences in ductility since this depended on maintaining a low temperature gradient as the specimen elongated in tertiary creep; also a double neck was formed in one specimen. Testing in air gave the same creep behaviour as the corresponding test *in vacuo*, although for the convenience of density measurements (see below) most of the tests were carried out *in vacuo*.

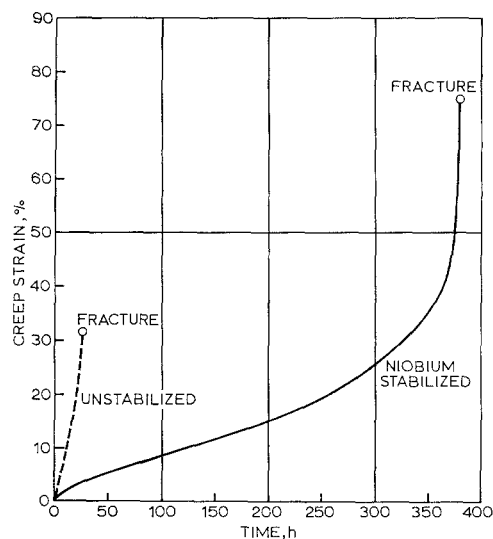


Figure 5 Creep curves for 20 Cr/25 Ni stainless steels showing effect of niobium on creep rate and ductility at 750° C.

Fig. 6 shows an Arrhenius plot for the fine-grained specimens tested at 62 MN m⁻². The slope of this line indicates an activation energy of 128 kcal mol⁻¹.

The creep resistance of the steel at 750° C is apparently related to the state of dispersion of the NbC precipitate. The finest dispersion, obtained by the 1250° C/820° C heat-treatment, gave the greatest creep resistance (table II) although the ductility was reduced and intergranular fracture occurred without necking. The strain to the onset of a tertiary ($\sim 20\%$) was the same as for the other specimens. A coarse

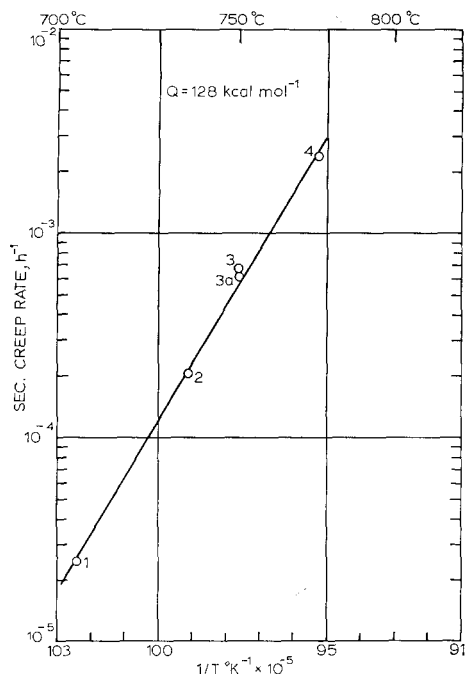


Figure 6 Temperature-dependence of creep rate.

precipitate of NbC, obtained by the 1250° C/1050° C heat-treatment, lowered the creep resistance significantly (table II).

2.4. Density Measurements

The specimens were removed from the creep apparatus at regular increments of strain and the fractional change in density between the specimen and its control, $\Delta D/D$, was determined in the way described previously. Differential density measurements are more sensitive than metallographic observations in detecting the presence of cavities. Fig. 7 shows results obtained on specimen 3 at 750° C. Similar results were obtained on the other fine-grained specimens and indicated that an appreciable density change ($\Delta D/D > -5 \times 10^{-5}$) was formed only near the end of secondary creep at strains greater than 15%. Metallographic examination of fractured specimens showed that cavities in these specimens were nucleated at NbC particles in the grains. In the necked region these cavities were considerably elongated, suggested that cavitation was incidental to and not the cause of fracture.

Density measurements on the coarse-grained specimen 6 again did not detect cavitation below 15% creep strain (fig. 8), although once nucleated the cavitation developed rapidly in tertiary

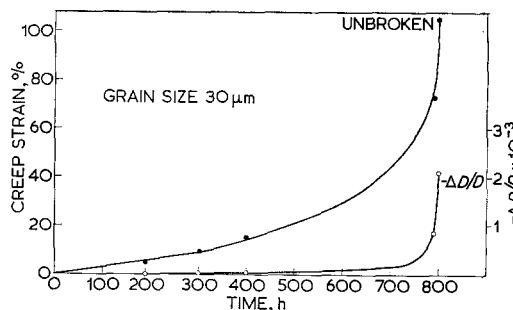


Figure 7 Variation of creep strain and $-\Delta D/D$ with time for fine-grained 20 Cr/25 Ni/Nb stainless steel at 750° C, 62 MN m⁻².

creep, limiting the ductility to 27%. Figs. 9a and b show that no simple time or strain relationship with $\Delta D/D$ is followed. Fig. 10 shows that both surface-cracks and wedge-cracks contributed to the observed density change. The contribution of surface-cracks was determined by testing a second specimen under the same conditions to 20% strain and then determining $\Delta D/D$ of the gauge length before and after machining 0.33 mm from the diameter. It was found that $\Delta D/D$ decreased from -2.04×10^{-3} to -1.54×10^{-3} after machining off the surface layer and from this it can be shown that $\Delta D/D$ for the surface layer was -3.58×10^{-3} . Surface-cracks therefore make an appreciable contribution to the density change in this instance.

In the large-grained specimens local grain boundary migration into the denuded zone was observed, mainly on boundaries inclined to the stress axis and, since this occurred only in the gauge length, the migration must be stress-induced. It can be seen in fig. 11 that the regions swept by this migration were free of precipitates

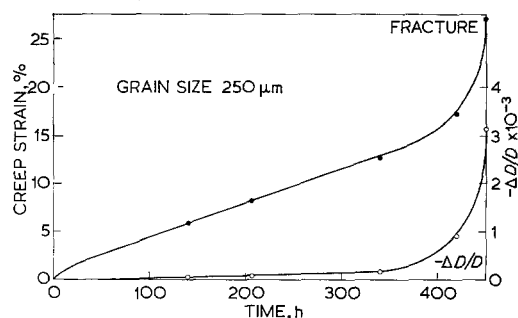


Figure 8 Variation of creep strain and $-\Delta D/D$ with time for coarse-grained 20 Cr/25 Ni/Nb stainless steel at 750° C, 93 MN m⁻².

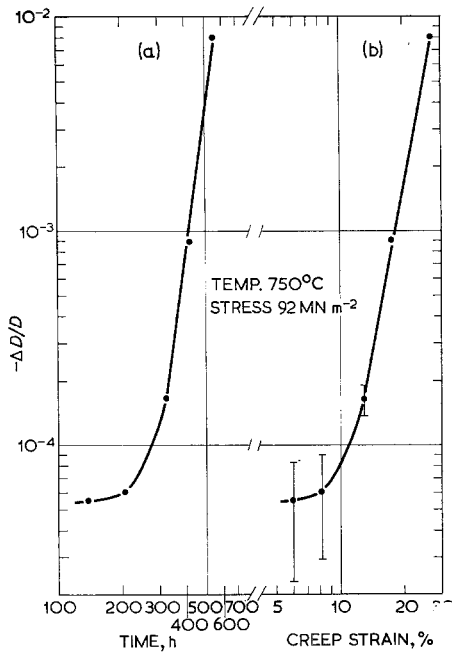


Figure 9 Variation of $-\Delta D/D$ with (a) time and (b) strain for coarse-grained specimen at 750°C , 93 MN m^{-2} .

and also that the grain boundary precipitate is coarser for the two boundaries showing denuded zones.

2.5. Measurement of Grain Boundary Sliding

A few surface measurements of grain boundary sliding were made on the fine-grained specimens to see whether the difference in cavitation behaviour between this steel and the niobium-free steel



Figure 10 Grain boundary cracks in the surface layer of large-grained specimen strained 27% to fracture at 750°C ($\times 82$).

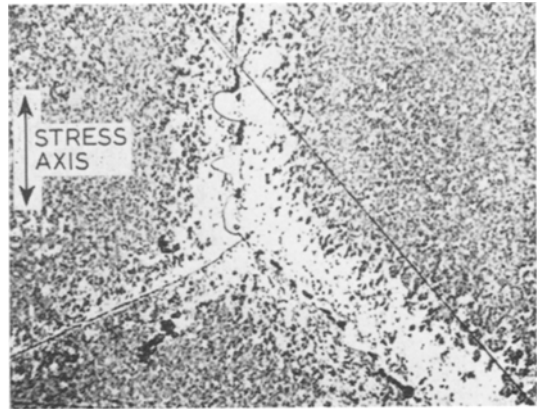


Figure 11 As fig. 10, showing grain boundary migration into the denuded zone. The inclined grain boundary contains both coarse NbC and discrete cavities ($\times 515$).

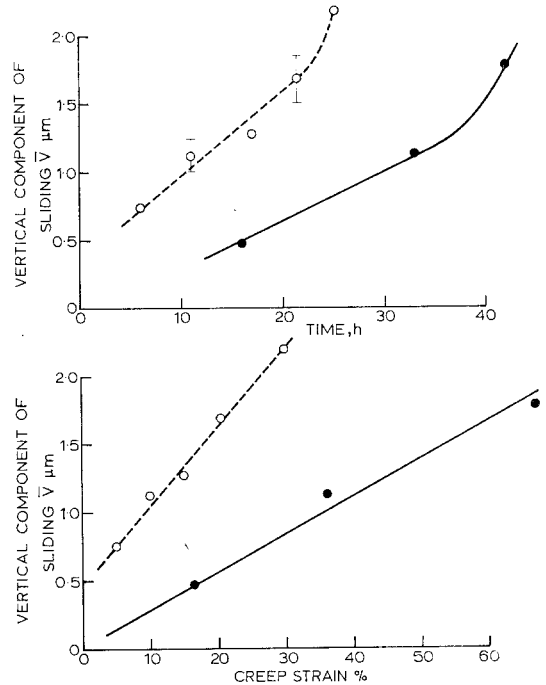


Figure 12 Grain boundary sliding as a function of, top, time and, bottom, strain for 20Cr/25Ni stainless steels at 750°C . Min. creep rate 10^{-2} h^{-1} . \circ --- \circ , 20/25/unst; stress 62 MN m^{-2} ; \bullet — \bullet 20/25/Nb; stress 93 MN m^{-2} .

used in the earlier work was caused by differences in the sliding behaviour. Comparison is made in fig. 12 between the two steels given the same heat-treatment and having the same grain size. The secondary creep rate was 10^{-2} h^{-1} for both specimens. At a given strain (or time) the amount of sliding in the niobium-stabilised steel

is 2 to 3 times less than in the unstabilised steel. The amount of sliding is small compared with the grain size so that the high ductilities of 20 Cr/25 Ni/Nb steels are not the result of large relative grain movements.

3. Discussion

The addition of a strong carbide-forming element to 20 Cr/25 Ni stainless steel leads to an improvement in both creep resistance and ductility. The creep resistance of the niobium-stabilised steel is shown to be related to the dispersion of NbC, the greatest creep resistance being associated with a fine dispersion.

The large activation energy at the relatively high strain rates (128 kcal mol⁻¹) compares with values of 70 kcal mol⁻¹ from long term creep data [5] and suggests that the activation energy is stress-dependent. A similar stress-dependence in a 16 Cr/16 Ni/Nb-stabilised austenitic steel observed by Russell *et al* [6] was attributed to a change in creep mechanism from cross-slip recovery at high stress to climb recovery and NbC/dislocation interaction at low stress.

The intrinsically high ductility of fine-grained 20 Cr/25 Ni steels containing niobium means that either it is difficult to nucleate cavities, or if small nuclei are formed at the beginning of the test they do not readily grow to a critical size. The nucleation of cracks at triple points has recently been considered by Smith and Barnby [7]. They modified the original Stroh [8] equation that was used by McLean [9] to predict the stress required to nucleate triple-point cracks. In Smith and Barnby's analysis the nucleation stress is given by

$$\tau = \left(\frac{3\pi\gamma_B G}{8(1-\nu)L} \right)^{\frac{1}{2}} \quad (1)$$

where γ_B is the grain boundary surface energy, G the shear modulus, ν Poisson's ratio and L the sliding distance.

Equation 1 indicates lower nucleation stresses than predicted by Stroh's analysis. If it is assumed that sliding is supported by an infinite amount of material then L is equivalent to the grain-edge length. However, in materials containing discontinuities along the grain boundary, such as particles, this assumption is unrealistic since stress concentrations will be set up at these points. If the stress concentrations, produced when sliding is held up by a finite amount of material, are not relaxed, then cracks will be nucleated at these particles. Smith and Barnby

[10] showed that for grain boundary particles $2c$ in diameter and a distance $2d$ apart the nucleation stress is given by:

$$\tau = \frac{\pi}{2} \left(\frac{c}{d} \right)^{\frac{3}{2}} \left(\frac{4\gamma G}{(1-\nu)d} \right)^{\frac{1}{2}} \quad (2)$$

provided $c \ll d$. This equation also indicates lower nucleation stresses than predicted by the Stroh equation.

The addition of niobium to a 20 Cr/25 Ni steel decreases the rate of grain boundary sliding, suggesting that NbC particles on the grain boundary are effective in reducing the stress concentrations at triple points. When estimated values for the constants are inserted into equation 1 (assuming $L =$ grain-edge length) the stress obtained is similar to that used in the creep tests. Therefore, if the effective sliding length is reduced to less than L by the NbC precipitate, triple-point cracking will not occur. It is then appropriate to consider the possibility that r-type cavities may be nucleated at particles according to equation 2. This will not occur if the distance between particles is sufficiently small or the interfacial energy sufficiently high. Cottrell [11] suggested that "wetting" particles will be less likely to nucleate cavities than "non-wetting" particles. The "wettability" relates to the atomic bonding between precipitate and matrix such that when the interfacial energy is low (wetting) the work of separation is high, while high interfacial energies (non-wetting) will result in relatively easy fracture of the interface.

Keown and Pickering [12] suggested that the "wettability" and hence the interfacial energy was related to the mis-match of the lattice spacings of the precipitate and matrix, particles with a high degree of mis-match being non-wetting. In keeping with this theory, they found that the tendency of different carbides in a $\frac{1}{2}\%$ Mo steel to nucleate cavities increased with the mis-match of the lattice spacings. However, in austenitic steels this correlation is not observed, for chromium carbides have a lower mis-match than niobium carbide and yet the niobium-stabilised steel is less susceptible to cavitation. The interfacial energy is therefore not a simple function of the mis-match across the interface.

If small cavity nuclei are formed in the fine-grained niobium-stabilised steel, growth to a stable size will occur only when the rate of sliding exceeds the rate of sintering [13]. Therefore it is not clear whether the absence of cavitation in

these steels results from difficulty of nucleation or growth.

The cracks in the large-grained specimen appeared to propagate rapidly across the transverse grain boundaries, in the way envisaged by Lindborg [14] until arrested temporarily at the next triple point. Instead of then growing along the inclined grain boundary, shear in the denuded zones caused the crack to re-form on the next triple point, and in this way a crack several facets long was formed (fig. 10). The high dislocation density resulting from shear in the denuded zones of inclined grain boundaries caused the boundary to migrate locally into the denuded zone (fig. 11).

The tendency for large-grained 20 Cr/25 Ni/Nb to fail by triple-point cracking was probably due to both the intrinsically high creep resistance after solution-treatment at 1250° C and to the formation of relatively weak denuded zones which caused the strain to be concentrated near the grain boundary regions. Also by increasing the grain size, more sliding per boundary may occur and the minimum stress required for wedge-cracking is reduced. Although failure occurred by wedge-cracking, it is necessary to explain why cracks do not form until the end of secondary creep. Williams [15] suggested that when the denuded zones are very wide, as in the present case, the stress concentrations at the triple point are more easily relaxed and nucleation is inhibited. Since the cracks are formed near the end of secondary creep, the initial growth will be stable and it is suggested that the point when they become unstable corresponds to the onset of tertiary creep. Consequently, the analysis of Williams [16] cannot be applied to the growth of these cracks.

4. Conclusions

In fine-grained 20 Cr/25 Ni/Nb stabilised stainless steel, cavities are not detectable before the

end of secondary creep and high ductilities are obtained. The absence of cavitation is attributed to a reduced rate of grain boundary sliding and to a possible low interfacial energy between the carbide and the matrix.

Denuded zones in coarse-grained specimens, solution-treated at 1250° C and aged at 820° C, caused the strain to be concentrated near grain boundaries during creep, leading to intergranular fracture and lower ductility.

Acknowledgement

The author is grateful to Mr J. Morrison UKAEA Springfields for supplying the steel used in this investigation. Thanks are due to Mr G. Willoughby for assistance with creep testing and to colleagues at CERL and BNL for valuable discussions. This paper is published by permission of the CEGB.

References

1. A. GITTINS, *J. Mater. Sci.* **5** (1970) 226.
2. J. S. WADDINGTON and K. LOFHOUSE, *J. Nucl. Mat.* **22** (1967) 205.
3. D. R. HARRIES, *J. Brit. Nucl. Eng. Soc.* **5** (1966) 74.
4. M. DEIGHTON, *J. Iron St. Inst.* **205** (1967) 535.
5. L. RARATY, private communication.
6. B. RUSSELL, R. K. HAM, J. M. SILCOCK, and G. WILLOUGHBY, *Met. Sci. J.* **2** (1968) 201.
7. E. SMITH, and J. T. BARNBY, *ibid* **1** (1967) 56.
8. A. N. STROH, *Adv. Phys.* **6** (1957) 418.
9. D. MCLEAN, *J. Inst. Met.* **85** (1956) 468.
10. E. SMITH and J. T. BARNBY, *Met. Sci. J.* **1** (1967) 1.
11. A. H. COTTRELL, "Structural Processes in Creep" (ISI, London, 1961) p. 101.
12. R. KEOWN and F. B. PICKERING, private communication.
13. J. E. HARRIS, *Trans. AIMME* **233** (1965) 1509.
14. U. LINDBORG, *Acta. Met.* **17** (1969) 157.
15. J. A. WILLIAMS, *ibid* **15** (1967) 1559.
16. *Idem*, *Phil. Mag.* **15** (1967) 1289.

Received 15 December and accepted 29 December 1969